

# Relationships Between the Vertical Structure of Deep Convection and Upper Tropospheric Humidity in the Tropics and Subtropics

Jonathon Wright<sup>1</sup>

Georgia Institute of Technology, Atlanta, GA

Andrew Dessler<sup>2</sup>

Goddard Space Flight Center, Greenbelt, MD

**Abstract.** Climate change due to the infrared water vapor feedback depends critically upon the upper tropospheric humidity distribution in the tropics and subtropics, yet this distribution remains one of the largest sources of uncertainty in current climate models. This uncertainty in water vapor feedback stems in large part from the relatively unknown factors governing moist convective outflow into the tropical upper troposphere. We present and evaluate a method for investigating the vertical structure and temporal evolution of tropical convective outflow using satellite remote sensing. Precipitation radar observations from the Tropical Rainfall Measuring Mission are binned according to altitude and radar reflectivity, and then connected to upper tropospheric water vapor measurements from the Atmospheric Infrared Sounder through the integration of a sophisticated trajectory model. Preliminary results are discussed, along with plans for future work.

## 1. Introduction

Water vapor is widely recognized as the dominant greenhouse gas, due both to its con-

tinuum absorption over much of the infrared spectrum and its abundance relative to other greenhouse gases. As such, a strong understanding of the ways in which it feeds back to anthropogenic increases of other greenhouse gases is vital to making accurate projections of future climate change. At present, how-

---

<sup>1</sup>jswright@eas.gatech.edu

<sup>2</sup>Project mentor. Also at University of Maryland, College Park, MD

ever, this feedback remains one of the largest sources of uncertainty in climate models, resulting in widely varying forecasts of future temperature change (Held and Soden, 2000).

The greenhouse effect results from the fundamental principle of conservation of energy: energy in equals energy out. Sunlight travels through the atmosphere, warming the surface of the earth, and the earth responds by emitting energy in the form of infrared radiation. This radiation does not reach the top of the atmosphere, however; instead, it is absorbed by constituents in the atmosphere, including water vapor. As a result, the energy balance at the top of the atmosphere is maintained by the emission of energy from an atmospheric layer roughly located in the middle of the troposphere (see, e.g., Held and Soden, 2000, for a more complete explanation). Given a linear lapse rate of temperature with height in the troposphere, this results in a surface temperature that is significantly higher than that required by the energy balance at the top of the atmosphere, thus giving Earth the climate we know today.

When additional greenhouse gases, such as  $\text{CO}_2$ , are expelled into the atmosphere, the atmosphere becomes even more opaque to outgoing radiation, effectively raising the level of emission. Assuming that the lapse rate remains constant or increases, this amplifies the greenhouse effect, increasing the temperature between the level of emission and the surface. Increased atmospheric temperatures lead to an increased capacity for water vapor in the atmosphere, which could in turn lead to increased water vapor, further strengthening the greenhouse effect. This process of increased temperature to increased water vapor is known as the water vapor feedback.

There is no guarantee that an increased atmospheric capacity for water vapor will ac-

tually lead to increased water vapor, however. In fact, current estimates of the strength of the feedback vary widely, from zero feedback (Lindzen, 1990), in which the effect of increased  $\text{CO}_2$  is not further exacerbated by an increase in water vapor, to the constant relative humidity case (Moller, 1963; Manabe and Wetherald, 1967), in which water vapor increases the impact of increased  $\text{CO}_2$  by about an additional 70%, to estimates that indicate an even stronger radiative feedback.

Climate models estimate that 35% of the water vapor feedback is due to water vapor in the tropical upper troposphere, with the remaining 65% spread across the extratropics, subtropics, and tropical troposphere below 500 mb (Held and Soden, 2000). Cold temperatures at these altitudes mean that a small change in total water vapor can have a large impact radiatively, since the change is actually large relative to saturation. The general distribution can be understood as a balance between outflow from upward convective motion and large scale subsidence. Convection transports air from the boundary layer to the upper troposphere rapidly (hours) on highly localized spatial scales, while subsidence returns it more slowly (weeks) over a large area.

The reality is more complicated. In fact, while variations in water vapor occur roughly in phase with convection over land, convection and the resultant changes in UTH occur 12 hours out of phase over ocean, due primarily to differences in convective structure (Soden, 2000). The problem is further exacerbated by the fact that convection can act as either a source or a sink for UTH (Kley et al., 2000). On the one hand, convective outflow of small ice particles and water droplets can lead to evaporation and moistening in the upper troposphere, yet the introduction of

larger particles and droplets may cause existing upper tropospheric water vapor to condense and precipitate, thereby drying the surrounding area. Despite the complicating factors, though, it is now widely recognized that the strength of the water vapor feedback is highly dependent on the responses of convective outflow into the upper troposphere to increased greenhouse gas concentrations.

To first order, the influence of convective detrainment of moisture into the tropical upper troposphere is governed by the temperature of the detraining layer, and current climate models parameterize it accordingly. There are other factors involved, though, such as mesoscale downdrafts, which can promote drying, or microphysical processes within the convective column itself. The strength of the simulated water vapor feedback is highly dependent on the chosen detrainment scheme, therefore these higher order terms could exert a large influence on model results (Held and Soden, 2000).

Most previous studies of convective detrainment in the UT fall into three broad categories:

- *In situ* studies, relying on accurate but highly localized measurements, and only able to study the evolution of detrained air in the very short term.
- Model studies, which can take place on large or small spatial and temporal scales, but rely on simplified physics and cannot represent the totality of natural processes.
- Satellite studies, limited until recently by a general lack of information on convective vertical structure and a relative paucity of water vapor observations with adequate spatial and temporal resolution.

Here, we use the Tropical Rainfall Measuring Mission (TRMM) Precipitation Radar (PR), which provides some information about convective vertical structure, in conjunction with water vapor measurements from the Atmospheric Infrared Sounder, which provides high-resolution, global measurements of water vapor from the surface to the tropopause. We link these observations using a sophisticated transport scheme, with the intention of evaluating the role of convective detrainment into the tropical UT in the water vapor feedback, with particular emphasis on the role of ice.

In Sections 2 and 3 we describe the data and method, respectively. We present preliminary results in Section 4, and conclude with a summary and outline of future work in Section 5.

## 2. Data

### 2.1. Convection

We use the 13.8 GHz precipitation radar (PR) instrument onboard the Tropical Rainfall Measuring Mission (TRMM) satellite to determine convective location, depth, and intensity. While the instrument is intended to study the three-dimensional structure and amount of rainfall, it also provides an unprecedented opportunity to study and characterize the structure and properties of convection throughout the tropics and subtropics (Kummerow et al., 1998, 2000).

We use the 2A25 algorithm volumetric radar reflectivities, which provide some aspects of the three-dimensional structure of convective systems (Kummerow et al., 2000). The reported data values are representative of the radar echo from water droplets and ice particles within a volume. Larger values indicate either larger droplets or larger concentrations

of smaller droplets.

2A25 data are provided on a vertical resolution of 250m at nadir, increasing to about 1 km at the maximum inclination of 17°. Horizontal resolution ranges from a pixel size of about 4.3 km at nadir to 5 km at maximum inclination (Kummerow et al., 1998, 2000). While these resolutions are likely to miss smaller convective systems, this study is primarily interested in larger-scale systems, for which the instrument is considered reliable (Heymsfield et al., 2003). 49 observations are recorded in a 215 km cross-track swath, and the same area is revisited once or twice per day (Negri et al., 2002).

## 2.2. Water Vapor

We obtain upper tropospheric water vapor values in the tropics and subtropics using observations from the Atmospheric Infrared Sounder (AIRS) onboard the EOS Aqua satellite. AIRS is actually a system of instruments, each of which plays a role in the retrieval process. The AIRS infrared spectrometer provides high vertical resolution temperature and humidity soundings under clear sky conditions from the surface into the upper troposphere. The AIRS visible and near infrared photometer provides diagnostic support, flagging clouds and surface changes within the field of view. In addition, three of fifteen channels of the Atmospheric Microwave Sounding Unit (AMSU) are primarily devoted to water vapor measurements, allowing retrievals to continue to take place even under partially cloudy conditions (Aumann et al., 2003). For a complete discussion of the AIRS retrieval mechanism through clouds, see Susskind et al. (2003).

The horizontal resolution of AIRS water vapor is 40.5 km at nadir, corresponding to nine gridded and averaged infrared spectrom-

eter measurements and one AMSU measurement, and the instrument provides global coverage twice daily (Aumann et al., 2003). The water vapor sounding is retrieved on 13 pressure levels between the surface and 100 mb, and is matched with a climatological profile in the stratosphere. The goal of the AIRS instrument team is to retrieve water vapor soundings to 10% accuracy within the troposphere, and preliminary validations indicate that the observations are close to that threshold. A dry bias of -3.7% is observed in the upper troposphere up to 300 mb relative to operational sondes, along with a dry bias of -13% relative to the European Centre for Medium-Range Weather Forecasts model reanalyses (Fetzer, 2003). Members of the AIRS science team expect water vapor in the forthcoming version 4 data release to be reliable up to 100 mb (A. Eldering, personal communication).

## 3. Method

### 3.1. Initialization

To begin the method, we scan observations of TRMM PR for deep convection. We have chosen a threshold altitude of 10 km to represent deep penetration, and have set a reflectivity threshold of 20 dBZ as in Petersen and Rutledge (2001), since it slightly exceeds the PR noise threshold of 17 dBZ (Kummerow et al., 2000).

We then estimate the potential temperature of this observation. Since the TRMM data provide only geometric height as a vertical coordinate, we use reanalysis geopotential heights from the National Centers for Environmental Prediction (NCEP). Temperature  $T$  is evaluated via the hydrostatic relation, where we have assumed dry air for simplicity:

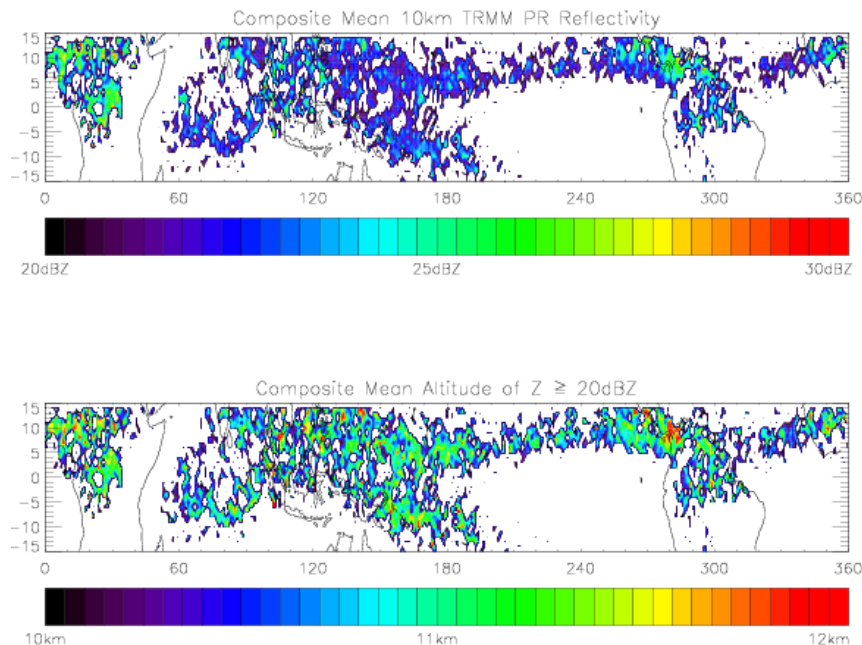


**Figure 1.** (a) July 2003  $1^\circ \times 1^\circ$  composite mean TRMM PR reflectivity at 10 km. (b) July 2003  $1^\circ \times 1^\circ$  composite mean altitude of radar reflectivities in excess of 20 dBZ.

$$T = -\frac{g}{R} \frac{\partial Z}{\partial \ln p} \quad (1)$$

where  $Z$  is the ERA-40 geopotential height,  $\ln p$  is the logarithm of the associated pressure level,  $g$  is the gravitational constant ( $9.81 m s^{-2}$ ), and  $R$  is the gas constant for dry air ( $287 m^2 s^{-2} K^{-1}$ ).

Potential temperature  $\theta$  is then calculated as:

$$\theta = T \left( \frac{1013 \text{ mb}}{p} \right)^\kappa \quad (2)$$

where 1013 mb represents average sea level pressure and  $\kappa = 2/7$ .

We assume equivalence between TRMM geometric height and NCEP geopotential height, and interpolate the potential temperature to each TRMM observation. We have also considered alternative methods for calculating

the potential temperature, and we will test the sensitivity of our choice of method in future work.

Figure 1 shows the locations and intensities of convection for July 2003. The intertropical convergence zone (ITCZ) is readily apparent, as is the monsoon region of South Asia. The most intense convection, in terms of both 10 km radar reflectivity and penetrating altitude, appears to be centered over equatorial Africa and Central America in the ITCZ. Note that the threshold altitude is 10 km, and that therefore this figure represents only those observations with  $Z \geq 20$  dBZ and  $z \geq 10$  km.

### 3.2. Trajectory Integration

Transport of the parcel from its initialization location is performed using the Goddard Fast Trajectory Model (Schoeberl and Morris, 2000; Morris and Schoeberl, 2003).

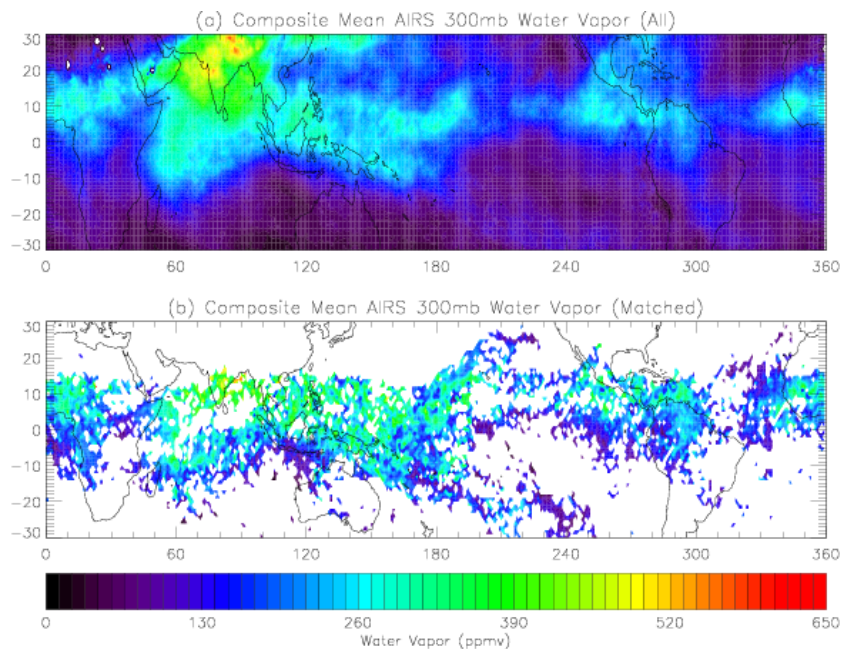


**Figure 2.** (a) July 2003  $1^\circ \times 1^\circ$  composite mean AIRS 300 mb water vapor. (b) July 2003  $1^\circ \times 1^\circ$  composite mean AIRS 300 mb water vapor matched backwards in time with TRMM PR observations of convection.

Horizontal and vertical motions are estimated along the trajectory path using diabatic calculations and winds from the United Kingdom Meteorological Office (UKMO) (Swinbank and O Niell, 1994). UKMO winds are updated daily at noon Universal Time (UT) on a  $2.5^\circ$  latitude  $\times$   $3.75^\circ$  longitude grid. Diabatic heating rates are calculated from the UKMO data via the radiative transfer model of Rosenfield et al. (1994).

The trajectory integration uses a timestep of one fiftieth of a day, or about 30 minutes, and winds and heating rates are interpolated to the trajectory point at each timestep. We store the spatial and temporal position of the trajectory at every timestep, resulting in an ensemble of trajectories with 251 points each, beginning at TRMM PR observations of deep convection and ending five days later.

### 3.3. Collocation

The overarching goal of this study is to connect convective detrainment with downstream water vapor. To this end, we scan the AIRS water vapor observations that are within 30 minutes of the trajectory passage. Spatial matches within these data are realized if one or more AIRS observations are within a  $1^\circ \times 1^\circ$  gridbox centered on the trajectory point. If the matching criteria result in multiple matches for a single trajectory point, we use the mean water vapor of all matched AIRS observations. Data are linearly interpolated from the AIRS standard pressure levels to match the trajectory pressure.

While version 3.0 of the AIRS data does not provide validated land observations, we have chosen to include them unvalidated in this analysis. We feel that the results of this

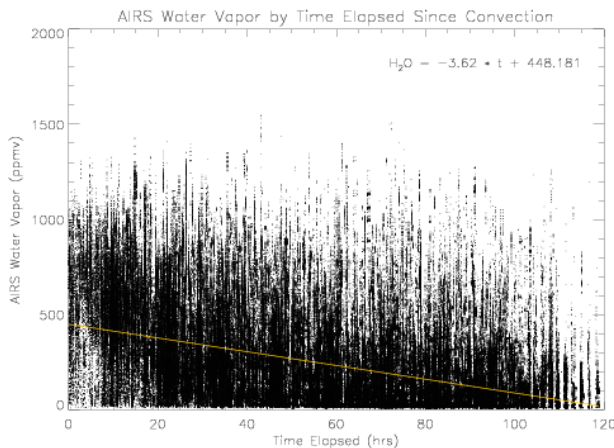


**Figure 3.** Water vapor evolution with time elapsed since convection. The yellow line represents the linear regression of water vapor with respect to time.

inclusion more closely represent those that will be attainable when we undertake longer term studies using version 4.0. The composite mean 300 mb water vapor for all of July 2003 is shown in figure 2a, while figure 2b shows the composite mean 300 mb water vapor for all matched observations during July 2003.

## 4. Results

It must be noted at this point that the results and analysis presented here are only preliminary. In particular, we have not yet sufficiently isolated height effects from intensity effects and vice versa. With this in mind, we present the following as examples of the types of analysis we have in mind for future study, with the intention of refining them substantially before completion of the final research product.

Figure 3 shows all upper tropospheric (400 mb-150 mb) matched water vapor values vs. the time elapsed since convection. We have

calculated a linear regression of water vapor vs. time, indicating an average dehydration rate of  $3.62 \pm 0.0068$  ppmv  $\text{hr}^{-1}$  and a mean initial outflow mixing ratio of  $448.181 \pm 0.26$  ppmv.

Figures 4a and 4b show the distribution of AIRS water vapor mixing ratios binned according to the altitude of the initial TRMM observation for days 1 and 5 of the trajectory integration, respectively. Preferential outflow altitudes are apparent in both panels, as well as in Figure 5. Here we have calculated linear regressions of vapor in time, as in Figure 3, while binning all matches according to the initial outflow altitude. The solid blue line represents the intercept, or average time 0 outflow mixing ratio, while the dashed red line represents the slope, or average dehydration rate.

Peaks in outflow mixing ratio and dehydration rate appear to occur together at 10.75 km, 12.25 km, 14.25 km and 16.5 km. The peak near 14 km corresponds to the accepted base of the tropical tropopause layer (TTL) (Highwood and Hoskins, 1998; Folkins et al., 1999; Alcala and Dessler, 2002), and it is also interesting to note the increase in dehydration rate relative to the outflow mixing ratio at this altitude. Preliminary indications using sample sizes at each altitude bin indicate that the peaks at 14.25 km and 16.5 km are generally occurring at the tops of convective systems, while those at 10.75 km and 12.25 km are not. Regardless, we will focus on each of these peaks separately in future work, with the following questions in mind:

- What types of convection are occurring at each peak?
- What regions are these convective systems occurring in?

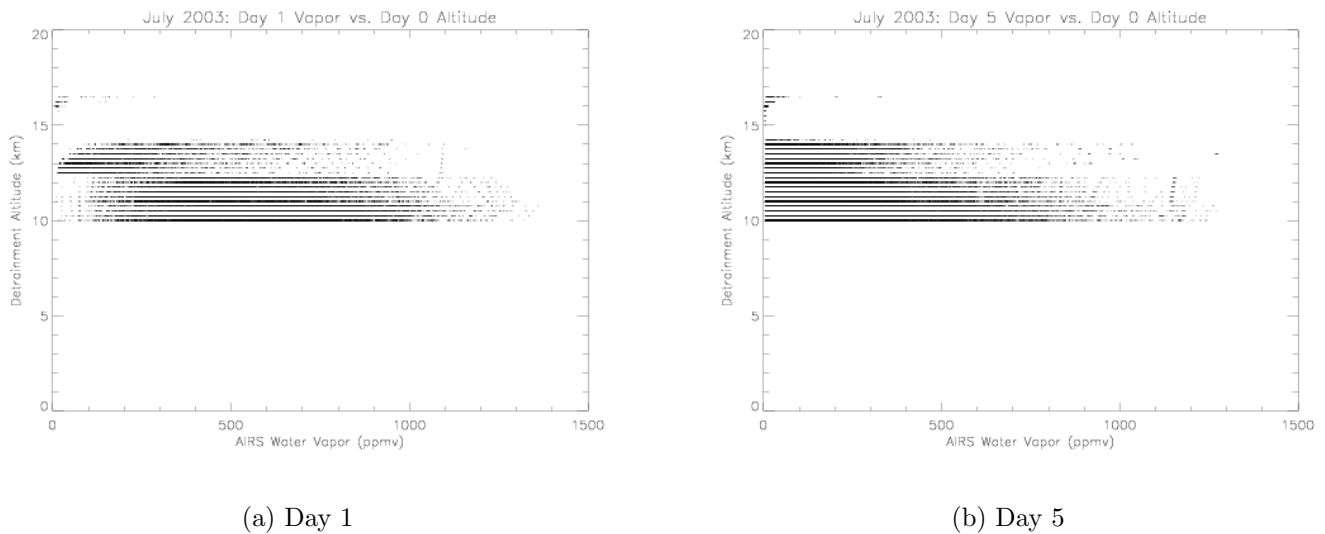


**Figure 4.** (a) All AIRS water vapor observations matched on day 1 of the trajectory binned by the altitude of the original TRMM observation. (b) Same as (a), but for day 5 of the trajectory.

- How high does the system typically penetrate?
- What role does seasonal variability play?

Figures 6a and 6b show the distribution of AIRS water vapor mixing ratios binned according to the reflectivity of the initial TRMM observation for days 1 and 5 of the trajectory integration, respectively. On day 1, the general shape of the distribution approximates the area under a bell curve, while on day 5, the outline has changed to more of a negative exponential curve. This immediately begs the question: Is air detrained from higher reflectivities dehydrating more quickly?

Figure 7 shows the same quantities as Figure 5, but the bins are now 1 dBZ reflectivity bins rather than 250 m height bins. It appears that dehydration rate may increase, but only above about 35 dBZ. It is also notable that dehydration rate seems to increase relative to outflow mixing ratio. This may indicate that,

at the droplet sizes represented by these reflectivities, vapor is more likely to condense onto droplets and precipitate out.

## 5. Discussion and Future Work

Overall, we feel that the method and data described here show significant potential for further study. It must be emphasized again that all of the preceding results are preliminary, and that at this point the variables are not sufficiently independent for clear conclusions. Instead, we mark several intriguing results for future study:

- Downstream UTH varies much more strongly with outflow altitude than with the intensity/reflectivity of convection.
- We observe four apparent peaks in downstream water vapor vs. detrainment altitude.

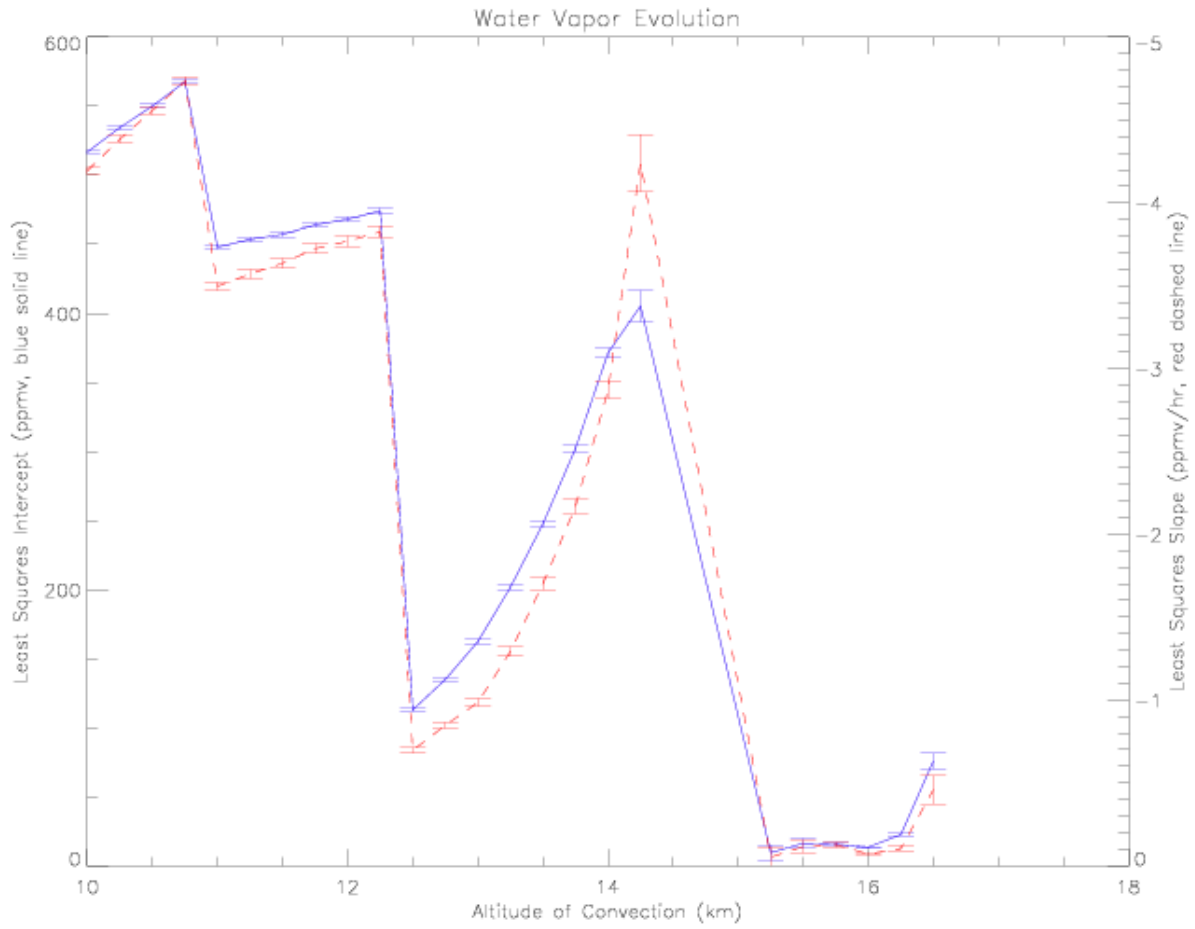
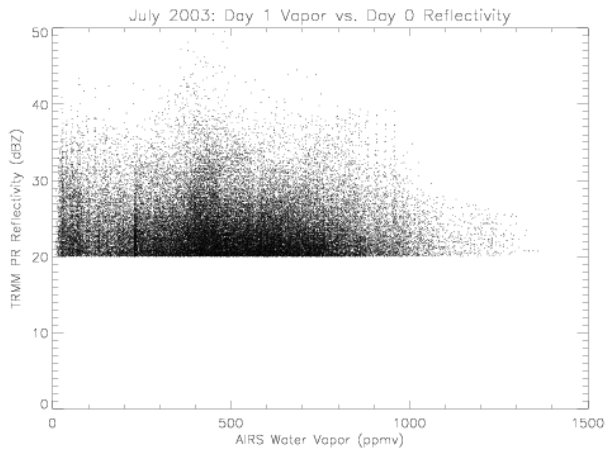
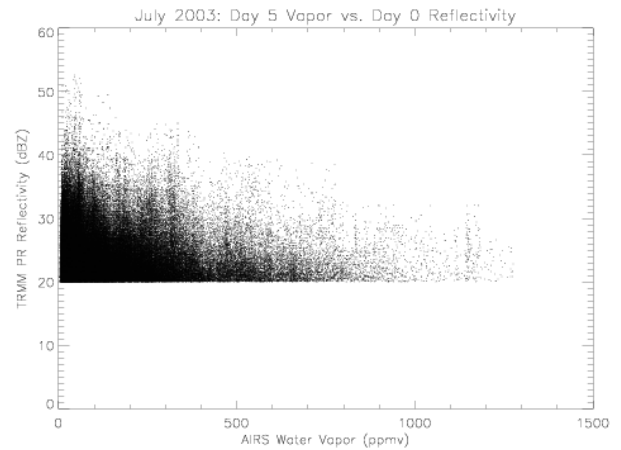


**Figure 5.** Least squares slopes (dashed red) and intercepts (solid blue) for trajectory points matched to outflow altitudes within 250 m height bins. Linear regressions are calculated in the same way as that shown in Figure 3.



(a) Day 1



(b) Day 5

**Figure 6.** As in Figure 4, but binned by the reflectivity of the original TRMM observation.

- Dehydration rate and outflow mixing ratio decrease together as reflectivity increases from 20 dBZ to 35 dBZ, then increase, with dehydration rate appearing to increase relative to outflow humidity as well.

In addition, while we have not yet had the opportunity to test the sensitivity of the method to various parameters, we intend to do this rigorously in the near future. The method will also be modified to accommodate the forthcoming AIRS version 4 data product, as well as a longer term study. We will investigate seasonal and regional variability within this framework, and develop analysis techniques that more fully isolate the variables and provide for more robust conclusions. We will initiate appropriate case studies, such as coincidence of TRMM observations with aircraft studies, and link observations within convective systems. This will provide a more complete representation of each system and assist in the validation of results.

**Acknowledgments.** We are grateful to Rong Fu for helpful suggestions, and Alison Walker, Mingxuan Chen, and Walter Petersen for programming assistance.

## References

- Alcala, C. and A. Dessler, 2002: Observations of deep convection in the tropics using the Tropical Rainfall Measuring Mission (TRMM) precipitation radar. *J. Geophys. Res.*, **107**.
- Aumann, H., M. Chahine, C. Gautier, M. Goldberg, E. Kalnay, L. McMillin, H. Revercomb, P. Rosenkranz, W. Smith, D. Staelin, L. Strow, and J. Susskind, 2003: AIRS/AMSU/HSB on the Aqua mission: design, science objectives, data products, and processing systems. *IEEE Trans. Geosci. Remote Sensing*, **41**, 253–264.
- Fetzer, E., 2003: Validation of AIRS/AMSU/HSB core products for data release version 3.0. Technical Report JPL D-26538, Jet Propulsion Laboratory, Pasadena, CA.

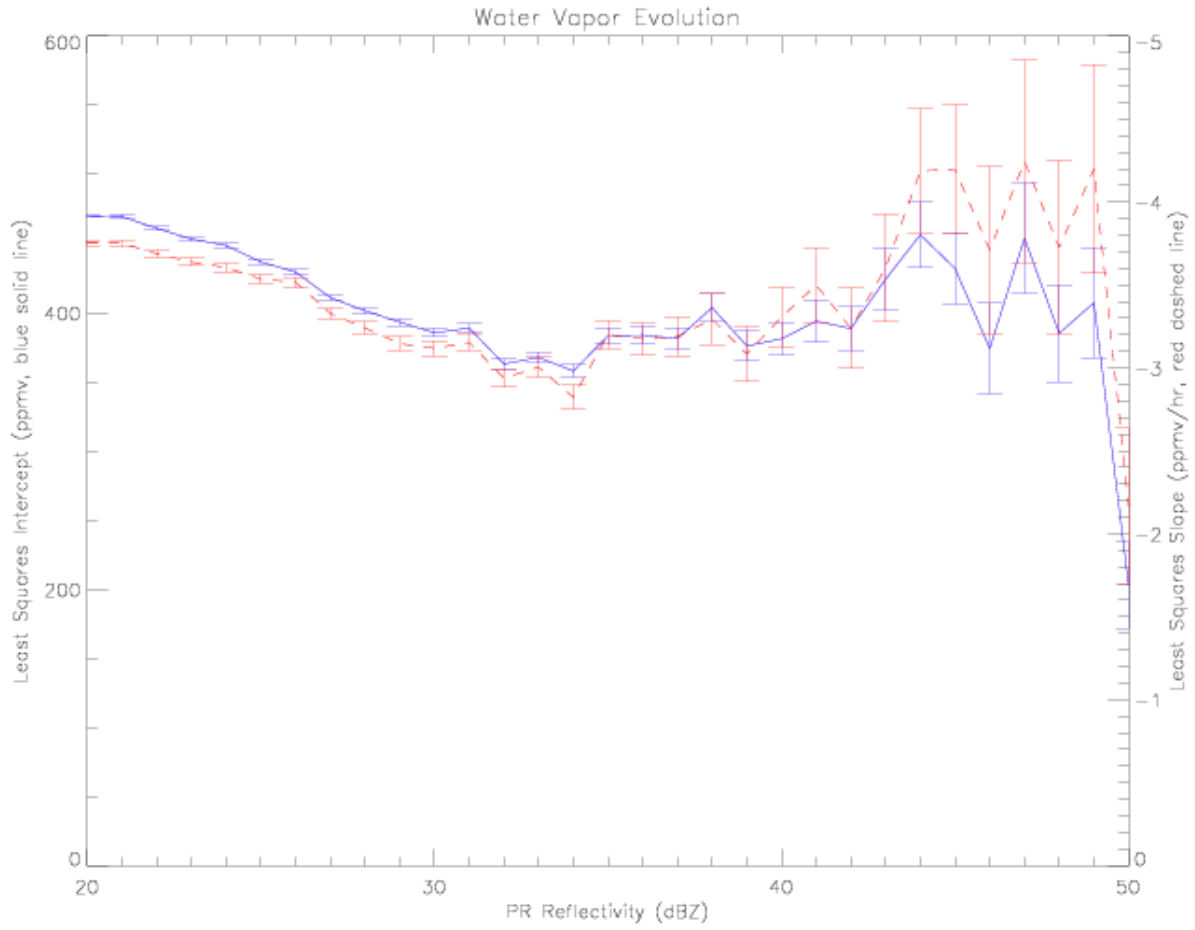


**Figure 7.** As in Figure 5, but for trajectory points matched to outflow reflectivities within 1 dBZ reflectivity bins.

- Folkins, I., M. Loewenstein, J. Podolske, S. Oltmans, and M. Proffitt, 1999: A barrier to vertical mixing at 14 km in the tropics: evidence from ozonesondes and aircraft measurements. *J. Geophys. Res.*, **104**, 22095–22102.
- Held, I. and B. Soden, 2000: Water vapor feedback and global warming. *Annu. Rev. Energy Environ.*, **25**, 441–475.
- Heymsfield, G., B. Geerts, and L. Tian, 2003: TRMM precipitation radar reflectivity profiles compared to high-resolution airborne and ground-based measurements. *J. Appl. Meteor.*, **42**, 769–774.
- Highwood, E. and B. Hoskins, 1998: The tropical tropopause. *Q. J. R. Meteorol. Soc.*, **124**, 1579–1604.
- Kley, D., J. Russell III, and C. E. Philips, 2000: SPARC assessment of upper tropospheric and stratospheric water vapor. Technical Report WCRP-113, WMO/TD-No.1043, World Meteorol. Organ., Geneva.
- Kummerow, C., W. Barnes, T. Kozu, J. Shuie, and J. Simpson, 1998: The Tropical Rainfall Measuring Mission (TRMM) sensor package. *J. Atmos. Oceanic Technol.*, **15**, 809–817.
- Kummerow, C., J. Simpson, O. Thiele, W. Barnes, A. Chang, E. Stocker, R. Adler, A. Hou, R. Kakar, F. Wentz, P. Ashcroft, T. Kozu, Y. Hong, K. Okamoto, T. Iguchi, H. Kuroiwa, E. Im, Z. Haddad, G. Huffman, B. Ferrier, W. Olson, E. Zipser, E. Smith, T. Wilheit, G. North, T. Krishnamurthi, and K. Nakamura, 2000: The status of the Tropical Rainfall Measuring Mission (TRMM) after two years in orbit. *J. Appl. Meteor.*, **39**, 1965–1982.
- Lindzen, R., 1990: Some coolness concerning global warming. *Bull. Am. Meteorol. Soc.*, **71**, 288–299.
- Manabe, S. and R. Wetherald, 1967: Thermal equilibrium of the atmosphere with a given distribution of relative humidity. *J. Atmos. Sci.*, **24**, 241–259.
- Moller, F., 1963: On the influence of changes in CO<sub>2</sub> concentration in air on the radiation balance of Earth’s surface and on climate. *J. Geophys. Res.*, **68**, 3877–3886.
- Morris, G. and M. Schoeberl, 2003: Potential impact of subsonic and supersonic aircraft exhaust on water vapor in the lower stratosphere assessed via a trajectory model. *J. Geophys. Res.*, **108**, doi:10.1029/2002JD002614.
- Negri, A., T. Bell, and L. Xu, 2002: Sampling of the diurnal cycle of precipitation using TRMM. *J. Atmos. Ocean Technol.*, **19**, 1333–1344.
- Petersen, W. and S. Rutledge, 2001: Regional variability in tropical convection: observations from TRMM. *J. Clim.*, **14**, 3566–3586.
- Rosenfield, J., P. Newman, and M. Schoeberl, 1994: Computations of diabatic descent in the stratospheric polar vortex. *J. Geophys. Res.*, **99**, 16,677–16,689.
- Schoeberl, M. and G. Morris, 2000: A Lagrangian simulation of supersonic and subsonic aircraft exhaust emissions. *J. Geophys. Res.*, **105**, 11,833–11,839.
- Soden, B., 2000: The diurnal cycle of convection, clouds, and water vapor in the tropical upper troposphere. *Geophys. Res. Lett.*, **27**, 2173–2176.
- Susskind, J., C. Barnet, and J. Blaisdell, 2003: Retrieval of atmospheric and surface parameters from AIRS/AMSU/HSB data in the presence of clouds. *IEEE Trans. Geosci. Remote Sensing*, **41**, 390–409.
- Swinbank, R. and A. O Niell, 1994: A stratosphere-troposphere data assimilation system. *Mon. Weather Rev.*, **122**, 686–702.